J. Fluid Mech. (2008), *vol.* 617, *pp.* 207–229.
doi:10.1017/S0022112008003923 Printed in the United Kingdom

A paradox of hovering insects in two-dimensional space

MAKOTO IIMA†

Research Institute for Electronic Science, Hokkaido University, N12W6, Sapporo, 060-0812, Japan

(Received 6 February 2008 and in revised form 21 August 2008)

A paradox concerning the flight of insects in two-dimensional space is identified: insects maintaining their bodies in a particular position (hovering) cannot, on average, generate hydrodynamic force if the induced flow is temporally periodic and converges to rest at infinity. This paradox is derived by using the far-field representation of periodic flow and the generalized Blasius formula, an exact formula for a force that acts on a moving body, based on the incompressible Navier–Stokes equations. Using this formula, the time-averaged force can be calculated solely in terms of the time-averaged far-field flow. A straightforward calculation represents the averaged force acting on an insect under a uniform flow, $-\langle V \rangle$, determined by the balance between the hydrodynamic force and an external force such as gravity. The averaged force converges to zero in the limit $\langle V \rangle \to 0$, which implies that insects in two-dimensional space cannot hover under any finite external force if the direction of the uniform flow has a component parallel to the external force. This paradox provides insight into the effect of the singular behaviour of the flow around hovering insects: the far-field wake covers the whole space. On the basis of these assumptions, the relationship between this paradox and real insects that actually achieve hovering is discussed.

1. Introduction

Theoretical studies of animal locomotion in fluids based on fundamental equations have thus far been limited to cases where the fluid flow has a low Reynolds number or where the flow is inviscid (Childress 1981). Although it is possible to evaluate exactly the hydrodynamic force generated by steady wings, this calculation is not possible in the case of flying insects, even if details of the wing properties and the flapping motion are provided. Insects flap their wings periodically to generate vortices separated from the wing; these are essential to achieve high performance in force generation and manoeuvring (Dudley 2000). However, this induced flow is unsteady and rotational, characteristics that are outside the scope of wing theory. From experimental observations, several flapping-flight mechanisms for insects have been proposed to explain particular local interactions between separation vortices and wings: the Weis-Fogh mechanism (Weis-Fogh 1973; Maxworthy 1979; Edwards & Cheng 1982), the delayed stall mechanism (Dickinson & Götz 1993; Ellington *et al.* 1996), and the wake capture mechanism (Dickinson, Lehmann & Sane 1999; Sane & Dickinson 2002). The generated hydrodynamic force is theoretically evaluated by applying quasi-steady-state assumptions with typical values of the lift and drag coefficients for moving wings (Dickinson *et al.* 1999; Wang, Birch & Dickinson

† Email address for correspondence: makoto@nsc.es.hokudai.ac.jp

2004), the single-vortex approximation based on inviscid fluid behaviour (Edwards & Cheng 1982), or direct numerical simulation (Liu *et al.* 1998; Wang *et al.* 2004; Iima 2007). An analysis of related problems can be found, for example, in Childress, Vandenberghe & Zhang (2006) and Pesavento & Wang (2004). However, owing to the complexity of analysing the mechanism of vortex separation and the dynamics of the separation vortices, no theory that is purely based on the Navier–Stokes equations for flapping flight using vortices, without relying on numerical calculation, has thus far been proposed, although the flow around a body oscillating with small amplitude has been analysed (Riley 1967).

This difficulty can be overcome for the flapping flight of insects by focusing on the far-field flow. Several authors have derived exact unsteady force formulae in two- and three-dimensional space by calculating the rate of change of momentum in a controlled volume (Imai 1974; Noca, Shiels & Jeon 1997; Wu, Pan & Lu 2005). Such formulae make evaluation of the force acting on a body moving through a fluid governed by the Navier–Stokes equations possible. In particular, Imai (1974) proposed a generalized Blasius formula in two-dimensional space, by which the unsteady force can be calculated in terms of only an integral on the control surface, which can be chosen in the far field, and an integral on the body surface. A three-dimensional formula with the same properties was proposed by Wu *et al.* (2005). Because the far-field flow can be evaluated using the Oseen equation (Chadwick 1998; Chadwick & Fishwick 2007), for which a general solution is obtained, the unsteady force generated by flapping wings can be evaluated even if separation vortices are formed.

Several two-dimensional models for insect free-flight have a universal structure for the critical point near hovering, suggesting a singularity. A model that involves two wings flapping vertically (Iima & Yanagita 2001*a*, *b*, 2005, 2006) as is commonly observed during butterfly hovering (Ellington 1984; Betts & Wootton 1988), has been studied numerically. The centre of mass (CM) of the model is allowed to move along a vertical line, according to the hydrodynamic force generated by the separation vortices and the external force (gravity). It has been shown that hovering is impossible in this model in the following sense: if the magnitude of the external force is arranged such that the CM velocity approaches zero, the model loses stability when the CM velocity falls below a critical value, being attracted to another steady state with a CM velocity of opposite sign. (Iima & Yanagita 2006). Another model involving a single wing flapping horizontally (Iima 2007), as observed during the hovering of many insects (Ellington 1984; Dudley 2000), yields qualitatively the same result, although the flapping motion and generated vortex pattern are qualitatively different (Iima 2007). These numerical results suggest that there exists some singularity in two-dimensional hovering; however, no theoretical argument to this effect has yet been presented.

In this paper, a paradox for the force acting on a hovering insect is proposed in order to discuss the singularity. If the period-averaged velocity of the insect ($\langle V \rangle$) is constant, the period-averaged force acting on the insect ($\langle F \rangle$) can be evaluated by considering the force generated by a flapping wing under a uniform flow of $-\langle V \rangle$. Assuming that the flow is temporally periodic and converges to $-\langle V \rangle$ at infinity, it is shown that $\langle F \rangle$ converges to zero as $\sim (\log |\langle V \rangle|)^{-1}$ in the limit of hovering: $\langle V \rangle \to 0$. This result appears paradoxical because, in reality, insects look as though they are hovering when $\langle V \rangle$ is zero. This paradox provides insight into the necessary criteria for hovering.

This paper is organized as follows. Section 2 is devoted to explaining the physical aspects of the problem to be proved mathematically in the subsequent sections. The far-field flow for a flying insect is obtained in § 3 as a general form of the far-field

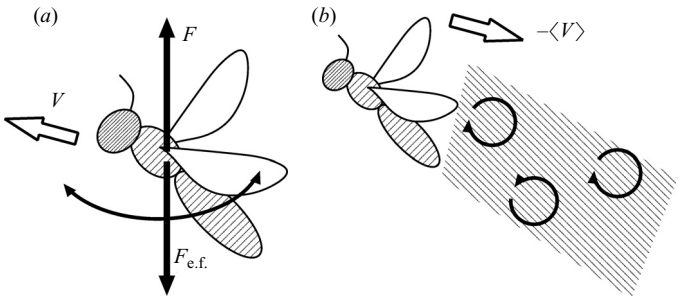

FIGURE 1. (*a*) Configuration of the problem: an insect flies in a two-dimensional space under an external force. A steady state is assumed. (*b*) Movement of the coordinate with the averaged velocity. For this coordinate, the insect is stationary under a uniform flow $-\langle V \rangle$. Because of the steady-state assumption, the flow induced by the flapping motion is periodic in this coordinate. The vortices generated are drawn schematically.

flow for an oscillating body. The average force acting on the insect is obtained in § 4 using the far-field flow and a generalized Blasius formula. In § 5, the limit of the averaged force is calculated, leading to the theoretical paradox. In § 6, the factors that enable real insects to hover are discussed, based on the assumptions that lead to the paradox. The validity of the assumptions required for this calculation is evaluated in terms of fluid mechanics and biology. Because a proof of the generalized Blasius formula for the force has not been given in the literature (Imai 1974), this is provided in the Appendix.

2. Configuration and physical arguments

2.1. *Problem*

We consider an insect in two-dimensional space flying under the influence of a constant external force, $\boldsymbol{F}_{\mathrm{e.f.}}$, such as gravity. The wing of the insect generates separation vortices, by which it generates the unsteady hydrodynamic force $\boldsymbol{F}$. The velocity of the insect's CM, $\boldsymbol{V}$, is determined by the equation of motion:

$$M\frac{\mathrm{d}\boldsymbol{V}}{\mathrm{d}t} = \boldsymbol{F} + \boldsymbol{F}_{\mathrm{e.f.}}, \tag{2.1}$$

where M is the total mass of the insect (figure 1*a*).

Here, we assume steady-state conditions, for which $\boldsymbol{V}$, $\boldsymbol{F}$, and the flapping motion are temporally periodic. The period-average of (2.1) gives the following expression:

$$\boldsymbol{0} = M\frac{\mathrm{d}\langle \boldsymbol{V} \rangle}{\mathrm{d}t} = \langle \boldsymbol{F} \rangle + \boldsymbol{F}_{\mathrm{e.f.}}, \tag{2.2}$$

where $\langle * \rangle \equiv (1/T)\int_t^{t+T} * \mathrm{d}t$ denotes the period-average (T is the period). Here, we consider flight where a component of the uniform flow is parallel to a non-zero external force, that is, $\boldsymbol{F}_{\mathrm{e.f.}} \cdot \langle \boldsymbol{V} \rangle \neq 0$ if $\langle \boldsymbol{V} \rangle \neq 0$. We address the question of whether the averaged velocity ($\langle \boldsymbol{V} \rangle$) can be zero or asymptotically zero, if we control both the flapping motion ($\boldsymbol{F}$) and the non-zero external force ($\boldsymbol{F}_{\mathrm{e.f.}}$). Although the answer might seem to be in the affirmative at first glance, even for the two-dimensional case, analytical calculation based on the Navier–Stokes equations leads to a negative conclusion. This is the paradox presented in this paper. Although a detailed derivation is given in the following sections, an intuitive argument based on the geometry of the

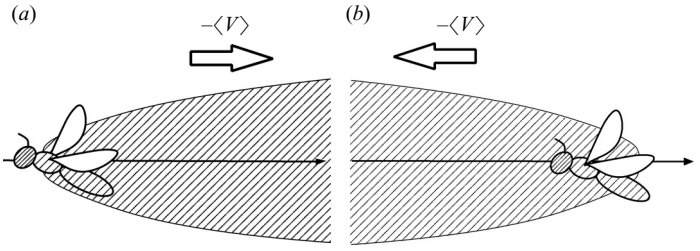

FIGURE 2. Schematic diagram of the wake. (*a*) The case in which the velocity of the uniform flow is positive. The wake is generated in the positive x-direction. (*b*) The case in which the velocity of the uniform flow is negative. The wake is generated in the negative x-direction.

wake structure, the region where vorticity cannot be disregarded, is useful to explain the essence of the paradox.

In a coordinate system moving with speed $\langle V\rangle$, the period-averaged position of the insect's CM is stationary (figure 1*b*). In this coordinate system, the insect is situated under a uniform flow $-\langle V\rangle$, and the flapping of its wings generates a vortex structure mainly in the downstream direction. In the far-field flow, where the flow is described by the Oseen equation, the vortex structures take the form of a parabolic wake, as shown in figure 2(*a*) (see also § 3). If we suppose that the direction of the uniform flow is opposite for some reason (for example, the sign of $\langle V\rangle$ is altered by controlling the flapping motion), then the direction of the wake is also reversed (figure 2*b*). Thus, a continuously changing $\langle V\rangle$ that crosses zero requires a directional change of the wake structure. However, when an insect achieves hovering in reality, that is, $\langle V\rangle = 0$, the vortex structure cannot be eliminated. The far-field is governed by the Stokes equation, and the wake covers the entire space in the sense that the vorticity decays as a power of r (§ 6.1.2). This implies that the wake structure is not parabolic. Because the averaged force is determined only by the far-field (§ 4), this wake structure may lead to anomalous behaviour of the averaged force.

2.2. *Basic equations*

We consider a two-dimensional incompressible flow. Let us assume that a wing of arbitrary form moves in an infinite space in a uniform flow of velocity $U = -\langle V\rangle$ streaming parallel to the x-axis. The boundary of the wing is denoted by B (figure 3). We assume that the wing moves periodically in time, and that the induced flow ($\boldsymbol{u}(\boldsymbol{x}, t)$) is also temporally periodic: $\boldsymbol{u}(\boldsymbol{x}, t) = \boldsymbol{u}(\boldsymbol{x}, t+T)$, where $T(<\infty)$ is the period. The flow velocity is also assumed to remain finite throughout the region occupied by the fluid. The flow is governed by the incompressible Navier–Stokes equations:

$$\frac{\partial \boldsymbol{u}}{\partial t} + (\boldsymbol{u}\cdot\nabla)\boldsymbol{u} = -\frac{1}{\rho}\nabla p + \nu\Delta\boldsymbol{u} + \boldsymbol{K}, \tag{2.3}$$

$$\nabla\cdot\boldsymbol{u} = 0, \tag{2.4}$$

where $\boldsymbol{u} = (u, v)$ is the velocity, ρ is the density, p is the pressure, ν is the kinematic viscosity, and $\nabla = (\partial/\partial x, \partial/\partial y)$. We assume that an external force $\boldsymbol{K}$ has a potential, and that $\boldsymbol{K}$ can be included in the pressure.

By taking the curl of (2.3), we obtain the vorticity equation:

$$\frac{\partial \omega}{\partial t} - \nu\Delta\omega = \frac{\partial(\Psi, \omega)}{\partial(x, y)}, \tag{2.5}$$

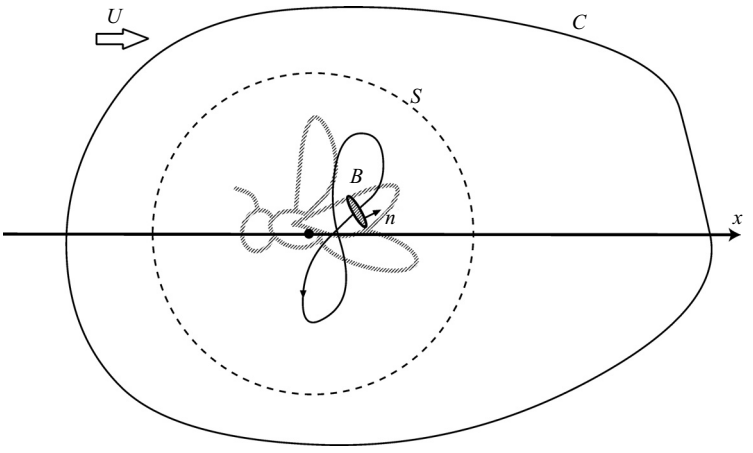

FIGURE 3. Configuration of the problem. A wing bounded by B moves periodically in a uniform flow. An arbitrary closed path including B is shown by C. A circle with a very large radius is indicated by the dotted line, where the region outside the circle is regarded as far-field in which the deviation of the flow velocity from $(U, 0)$ is small.

where $\omega = \partial v/\partial x - \partial u/\partial y$ is the vorticity and Ψ is a streamfunction such that:

$$u = \frac{\partial \Psi}{\partial y}, \quad v = -\frac{\partial \Psi}{\partial x} \tag{2.6}$$

(Imai 1951).

The period-averaged force, $\langle \boldsymbol{F} \rangle = (\langle F_x \rangle, \langle F_y \rangle)$, acting on B is given by:

$$\langle \boldsymbol{F} \rangle = \frac{1}{T} \int_t^{t+T} \boldsymbol{F} \, \mathrm{d}t, \quad \boldsymbol{F} = (F_x, F_y), \tag{2.7}$$

$$F_i = \iint_B \sigma_{ij}(t) n_j \, \mathrm{d}S \quad (i = x, y), \tag{2.8}$$

where $\sigma_{ij} = -p\delta_{ij} + \mu(\partial u_j/\partial x_i + \partial u_i/\partial x_j)$ is the component of the stress tensor $(u_x = u, u_y = v)$, $\mu = \rho\nu$ is the viscosity coefficient, $\boldsymbol{n} = (n_x, n_y)$ is the outward unit normal vector on B, and δ_{ij} is the Kronecker delta.

We aim first to obtain the expression for $\langle \boldsymbol{F} \rangle$ in terms of the characteristics of the far-field flow (§ 4), and secondly to calculate the asymptotic behaviour of $\langle \boldsymbol{F} \rangle$ as $U \to 0$ (§ 5).

3. Far-field flow for the flapping wing

3.1. *Far-field vorticity field: first approximation*

First, we consider the far-field flow from an oscillating body (the wing). We take the origin of the coordinate O at a point near the body and assume that the flow converges to a uniform flow, $(U, 0)$, such that:

$$\boldsymbol{u} = U\boldsymbol{e}_x + \boldsymbol{v}, \quad \lim_{|\boldsymbol{r}| \to \infty} \boldsymbol{v} = 0, \tag{3.1}$$

where $\boldsymbol{e}_x$ is a unit vector in the x-direction.

Taking a circle with a large radius (R) centred at O, we consider the equation for $\boldsymbol{v}$ outside the circle. Equation (3.1) implies that $|\boldsymbol{v}| \ll U$ for the region outside the

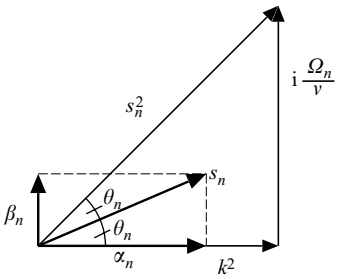

FIGURE 4. Relationship between k, Ω_n and s_n.

circle. If we write the streamfunction Ψ as

$$\Psi = Uy + \psi, \tag{3.2}$$

we obtain

$$\frac{\partial \omega}{\partial t} + 2\nu k \frac{\partial \omega}{\partial x} - \nu \Delta \omega = \frac{\partial(\psi, \omega)}{\partial(x, y)}, \tag{3.3}$$

where $k = U/2\nu$ and $\boldsymbol{v}$ is determined by ψ by the same relation as (2.6).

Assuming that ψ and ω are small, we introduce a small parameter ϵ which is of the order of $|\boldsymbol{v}|/U$, and expand ω and ψ as follows:

$$\omega = \epsilon\omega_1 + \epsilon^2\omega_2 + \epsilon^3\omega_3 + \cdots, \tag{3.4}$$

$$\psi = \epsilon\psi_1 + \epsilon^2\psi_2 + \epsilon^3\psi_3 + \cdots. \tag{3.5}$$

Substituting these equations into (3.3), and taking $O(\epsilon)$-terms, we obtain the Oseen equation:

$$\frac{\partial \omega_1}{\partial t} + 2\nu k \frac{\partial \omega_1}{\partial x} = \nu \Delta \omega_1. \tag{3.6}$$

The periodic solution of (3.6) is obtained by Fourier expansion. If we assume a periodic solution with a finite period T, $\omega_1(\boldsymbol{x}, t)$ is represented by

$$\omega_1(\boldsymbol{x}, t) = \sum_{n=-\infty}^{\infty} A_n(\boldsymbol{x}) \mathrm{e}^{\mathrm{i}\Omega_n t}, \quad \Omega_n = \frac{2\pi}{T} n \ \ (n \in \boldsymbol{Z}), \tag{3.7}$$

where $A_n(\boldsymbol{x}) = \overline{A}_{-n}(\boldsymbol{x})$ ($\overline{A}$ is the complex conjugate of A). If we write $A_n(\boldsymbol{x}) = B_n(\boldsymbol{x})e^{kx}$, the equation necessary to determine $B_n(\boldsymbol{x})$ is:

$$\left(\Delta - s_n^2\right) B_n = 0, \quad s_n^2 = k^2 + \mathrm{i}\frac{\Omega_n}{\nu}. \tag{3.8}$$

If $s_n = r_n \mathrm{e}^{\mathrm{i}\theta_n}$, we obtain $\mathrm{Re}(s_n) \equiv \alpha_n = r_n \cos\theta_n$ and $\mathrm{Im}(s_n) \equiv \beta_n = r_n \sin\theta_n$, where Re and Im denote the real and imaginary parts, respectively (figure 4).

We take $0 < \arg(s_n^2) < \pi/2$ such that $\alpha_n > 0$. For later convenience, we show that:

$$\alpha_n < \alpha_{n+1}. \tag{3.9}$$

The proof of this is as follows. First, the definition (3.8) gives $\mathrm{Re}(s_n^2) = \mathrm{Re}(s_{n+1}^2)$, which reduces to:

$$\alpha_n^2 - \alpha_{n+1}^2 = \beta_n^2 - \beta_{n+1}^2. \tag{3.10}$$

Because $\theta_n = (1/2)\tan^{-1}(\Omega_n/(\nu k^2))$, the inequality $\theta_{n+1} > \theta_n$ holds. The definition (3.8) gives $r_{n+1} > r_n$. Together, these inequalities give:

$$\beta_n = r_n \sin\theta_n < r_{n+1}\sin\theta_{n+1} = \beta_{n+1}. \tag{3.11}$$

The inequality (3.9) follows from (3.10) and the inequality (3.11).

Because $\alpha_n > 0$ and $k^2 = \mathrm{Re}(s_n^2) = \alpha_n^2 - \beta_n^2 \leqslant \alpha_n^2$, the following inequalities are obtained:

$$\alpha_n > 0, \quad \frac{\alpha_n}{k} \geqslant 1 \quad \text{(the equality holds only when } \beta_n = 0\text{)}. \tag{3.12}$$

The solution of (3.8) that satisfies $\lim_{|\boldsymbol{x}|\to\infty} B_n = 0$ is given as:

$$B_n(z) = \sum_{m=-\infty}^{\infty} R_{n,m} H_m^{(1)}(z)\mathrm{e}^{\mathrm{i}m\theta}, \ z = \mathrm{i}s_n r, \tag{3.13}$$

where $R_{n,m}$ are constants, $H_m^{(1)}$ is the Hankel function of the first kind, and (r,θ) is the position in polar coordinates. We note that the asymptotic form of $H_m^{(1)}$ is:

$$H_m^{(1)}(z) \sim \sqrt{\tfrac{2}{\pi z}}\exp\left[\mathrm{i}\left(z - \tfrac{1}{2}\pi m - \tfrac{1}{4}\pi\right)\right] \ (r\to\infty). \tag{3.14}$$

In summary, the periodic solution of (3.6) is given by:

$$\omega_1(\boldsymbol{x},t) = \sum_{n=-\infty}^{\infty}\sum_{m=-\infty}^{\infty} \omega_{m,n}(\boldsymbol{x},t), \tag{3.15}$$

$$\omega_{m,n}(\boldsymbol{x},t) = C_{m,n}\mathrm{e}^{\mathrm{i}\Omega_n t}\mathrm{e}^{kx}\mathrm{e}^{\mathrm{i}m\theta}H_m^{(1)}(z), \tag{3.16}$$

where $C_{m,n}$ are constants.

3.2. *Far-field wake region*

We obtain the wake region, i.e. the region where $\omega_{m,n}$ is significant, in the far region where the flow has been described well by (3.6).

Because $z = \mathrm{i}s_n r = \mathrm{i}\alpha_n r - \beta_n r$, $|H_m^{(1)}(z)| = |H_m^{(1)}(\mathrm{i}s_n r)| \leqslant C'|\sqrt{2/(\pi \mathrm{i} s_n)}\,|\,r^{-1/2}\exp(-\alpha_n r)$ for large r where C' is a constant. Using (3.16), and letting $p_n = \alpha_n/k$ and $x = r\cos\theta$, we obtain:

$$|\omega_{m,n}| \leqslant C_{max} r^{-1/2}\exp[-kr(p_n - \cos\theta)], \tag{3.17}$$

where $C_{max} = max_{m,n}|C'\sqrt{2/\pi\,\mathrm{i}\,s_n}C_{m,n}|$.

Let us consider the region defined by the inequality

$$kr(p_n - \cos\theta) < C, \tag{3.18}$$

where C is a constant. In this region (referred to hereinafter as the wake), $\omega_{m,n}$ is significant. Outside this region, $\omega_{m,n}$ decays faster than exponentially as r increases. Because $p_n \geqslant 1$ by the condition (3.12), the region determined by (3.18) is given as follows.

(i) *The case of* $p_n = 1$ $(n = 0)$

In this case, the mode $\omega_{m,0}$ corresponds to the solution of the steady Oseen equation. The boundary of the region determined by (3.18) is:

$$x = \frac{k}{2C}y^2 - \frac{C}{2k}, \tag{3.19}$$

which takes the form of a parabola (figure 5*a*). We note that the vorticity decays slowly ($\sim r^{-1/2}$) along the positive x-axis, but the contribution of this must be

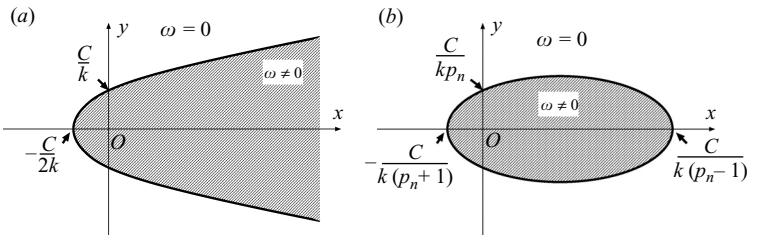

FIGURE 5. Wake regions for each mode (indicated by shading). (*a*) The case of $p_n = 1$. (*b*) The case of $p_n > 1$.

calculated. A similar situation occurs when calculating the drag acting on a body in a uniform flow, where the contribution of vorticity is significant (Imai 1951).

(ii) *The case of* $p_n > 1$ $(n \neq 0)$

The boundary of the region determined by (3.18) is:

$$k^2(p_n^2-1)\left\{x - \frac{C}{k(p_n^2-1)}\right\}^2 + k^2 p_n^2 y^2 = \frac{p_n^2}{p_n^2-1}C^2, \tag{3.20}$$

which is an ellipse (figure 5*b*).

The inclusion relation among $\mathscr{A}_n (n \geqslant 1)$, the wake determined by $\omega_{m,n}$, is:

$$\mathscr{A}_1 \supset \mathscr{A}_2 \supset \ldots, \tag{3.21}$$

which can be shown by using the inequality (3.9).

We now consider what happens to $\mathscr{A}_n$ in the limit $k \to 0$. Here, $\mathscr{A}_n (n \geqslant 1)$ is confined to a bounded region, which can be demonstrated as follows. We define that

$$l_n^{-1} \equiv \lim_{k\to 0} k p_n = \lim_{k\to 0} \alpha_n = \sqrt{\frac{\Omega_n}{2\nu}}, \tag{3.22}$$

and note that $l_n < l_1 = \sqrt{\nu T/\pi} < \infty$. Because $\mathscr{A}_n (n \geqslant 1)$ is included in the rectangular

$$\left[-\frac{C}{k(p_n+1)}, \frac{C}{k(p_n-1)}\right] \times \left[-\frac{C}{\sqrt{k^2(p_n^2-1)}}, \frac{C}{\sqrt{k^2(p_n^2-1)}}\right],$$

$\mathscr{A}_n (n \geqslant 1)$ is confined to the bounded region $[-Cl_1, Cl_1] \times [-Cl_1, Cl_1]$ in the limit $k \to 0$. However, the boundary of $\mathscr{A}_0$ diverges because k^{-1} diverges (see figure 5 and § 6.1.2 for the case where $k = 0 (\langle V \rangle = 0)$).

By using (3.15) and (3.16), we obtain:

$$\langle \omega_1 \rangle (\boldsymbol{x}) = \sum_{m=-\infty}^{\infty} \omega_{m,0}, \tag{3.23}$$

$$\omega_1'(\boldsymbol{x}, t) \equiv \omega(\boldsymbol{x}, t) - \langle \omega_1 \rangle (\boldsymbol{x}) = \sum_{n=-\infty, n\neq 0}^{\infty} \sum_{m=-\infty}^{\infty} \omega_{m,n}. \tag{3.24}$$

Therefore, the wake region for $\langle \omega_1 \rangle$ is inside the parabola $\mathscr{A}_0$, while the wake region for ω_1' is in the elliptical region $\mathscr{A}_1$. Outside these regions, $\langle \omega_1 \rangle$ and ω_1' reach zero at a faster than exponential rate as the distance from each region increases.

3.3. *Higher-order calculations*

Taking the $O(\epsilon^2)$-terms in (3.3) with the expansions (3.4) and (3.5), we obtain:

$$\frac{\partial \omega_2}{\partial t} + 2\nu k \frac{\partial \omega_2}{\partial x} - \nu \Delta \omega_2 = \frac{\partial(\psi_1, \omega_1)}{\partial(x, y)}. \tag{3.25}$$

The results given in § 3.2 indicate that ω_1' is significant only in the elliptical region $\mathscr{A}_1$. Therefore, we change the radius of the circle from R to R' such that the circle includes $\mathscr{A}_1$. Then, $\omega_1 \simeq \langle \omega_1 \rangle$ and $\psi_1 \simeq \langle \psi_1 \rangle$ outside the circle. Therefore, the flow outside the circle can be expressed by the following equation:

$$\frac{\partial \omega_2}{\partial t} + 2\nu k \frac{\partial \omega_2}{\partial x} - \nu \Delta \omega_2 = \frac{\partial(\langle \psi_1 \rangle, \langle \omega_1 \rangle)}{\partial(x, y)}. \tag{3.26}$$

Because the right-hand side of (3.26) does not vary with respect to time, the equation for ω_2' does not include the nonlinear term $\partial(\langle \psi_1 \rangle, \langle \omega_1 \rangle)/\partial(x, y)$. Therefore, ω_2' satisfies the same equation as (3.6), ω_2' is confined within an ellipse, and the expression for ω_2' is the same as (3.24). In this sense, it is necessary to consider only (3.24) for time-dependent vorticity fluctuations: ω_2' can be included in ω_1'.

For the time-averaged component, $\langle \omega_2 \rangle$, the higher-order equation is the same as that for the steady flow studied by Imai (1951). We can apply a similar analysis to the higher-order terms, enabling us to conclude that: first, the asymptotic behaviour for $\langle \omega \rangle$ is determined by the steady Navier–Stokes equation, and secondly, the region where ω' is significant is bounded. Outside this region, we can regard ω as equal to $\langle \omega \rangle$.

4. Averaged force acting on an insect with flapping wings

In this section, we give an exact formula for the averaged force acting on a periodically oscillating body in a viscous fluid by applying a generalized Blasius formula. To derive this result, we require an exact expression for the force acting on a body undergoing arbitrary motion in incompressible, unsteady, viscous and rotational flows.

The force $\boldsymbol{F}$ acting on a body undergoing arbitrary motion in a viscous fluid in two-dimensional space is given by Imai (1974) in the following complex form:

$$F = F_0 - \frac{\mathrm{d}}{\mathrm{d}t}\mathscr{P}, \tag{4.1}$$

$$F_0 = -\tfrac{1}{2}\mathrm{i}\rho \oint_C \overline{W}^2 \mathrm{d}\bar{z} - 2\mu \oint_C z \frac{\partial \omega}{\partial z}\mathrm{d}z + \mathrm{i}\rho \oint_C \omega z \mathrm{d}\Psi, \tag{4.2}$$

$$\mathscr{P} = -\mathrm{i}\rho \oint_C z W \mathrm{d}z - \rho \oint_B z \mathrm{d}\Psi, \tag{4.3}$$

where $F = F_x + \mathrm{i}F_y$, $W = u - \mathrm{i}v$ is the complex velocity, B is the boundary of the body, C is a time-independent arbitrary closed curve including the body, and S is the region bounded by B and C (figure 6). A proof for (4.1)–(4.3) is given in the Appendix. We note that all of these functions contain z and $\bar{z}$ as independent variables, meaning that W is not analytic in general because we consider the rotational flow. The relationship between W, Ψ and ω is:

$$W = 2\mathrm{i}\frac{\partial \Psi}{\partial z}, \quad \omega = -2\mathrm{i}\frac{\partial \overline{W}}{\partial z}, \tag{4.4}$$

which can be easily verified, as shown in the Appendix.

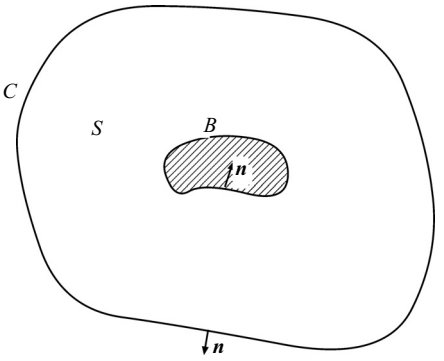

FIGURE 6. Schematic diagram of the body bounded by B, the control volume C, and the region bounded by B and C.

In this paper, we assume that the flow and the body motion are time-periodic with a finite period T. Any time-periodic function $F(\boldsymbol{x}, t)$ can be separated into the mean component,

$$\langle F\rangle(\boldsymbol{x}) \equiv \frac{1}{T}\int_t^{t+T} F(\boldsymbol{x}, t)\mathrm{d}t,$$

and the fluctuation component, $F' \equiv F - \langle F\rangle$:

$$F(\boldsymbol{x}, t) = \langle F\rangle(\boldsymbol{x}) + F'(\boldsymbol{x}, t). \tag{4.5}$$

If we assume that A and B are both time-periodic, then:

$$\langle AB\rangle = \langle A\rangle\langle B\rangle + \langle A'B'\rangle, \tag{4.6}$$

because $\langle A'\rangle = \langle B'\rangle = 0$.

When we assume that W, ω, Ψ and $\mathscr{P}$ are time-periodic, then separating W, ω and Ψ into their mean and fluctuation components, substituting them into (4.1)–(4.3), and using (4.6) gives:

$$\langle F\rangle = -\tfrac{1}{2}\mathrm{i}\rho\oint_C \langle\overline{W}\rangle^2\mathrm{d}\overline{z} - 2\mu\oint_C z\frac{\partial\langle\omega\rangle}{\partial z}\mathrm{d}z + \mathrm{i}\rho\oint_C \langle\omega\rangle z\langle\mathrm{d}\Psi\rangle$$
$$-\tfrac{1}{2}\mathrm{i}\rho\oint_C \langle\overline{W}'^2\rangle\mathrm{d}\overline{z} + \mathrm{i}\rho\oint_C z\langle\omega'\mathrm{d}\Psi'\rangle. \tag{4.7}$$

Because of the linear relationship between W and ω [(4.4)], $(\partial/\partial\overline{z})W' = -\mathrm{i}\omega'/2$. As was shown in § 3, ω' is significant only in the ellipse $\mathscr{A}_1$ in the sense that the value of ω' at a point (r, θ) outside $\mathscr{A}_1$ is bounded, because $|\omega'| < C'\exp(-kD'r)$, where C' and D' are constants. Thus, if we take C as a large circle with radius R that includes $\mathscr{A}_1$, we can assume that $\omega' = 0$ on C because the decay of ω' is bounded exponentially. Therefore, $(\partial/\partial\overline{z})W' = 0$ outside $\mathscr{A}_1$, which implies that W' satisfies the Cauchy–Riemann relation, $W' = W'(z, t)$. Because $W \to U$ as $r \to \infty$, $W' = a_1 z^{-1} + O(z^{-2})$. Therefore, we find that:

$$\oint_C \overline{W}'^2\mathrm{d}\overline{z} = 0. \tag{4.8}$$

Furthermore, because $\omega' = 0$ on C, then:

$$\mathrm{i}\rho\oint_C z\langle\omega'\mathrm{d}\Psi'\rangle = 0. \tag{4.9}$$

Thus, (4.7) can be simplified to:

$$\langle F\rangle = -\tfrac{1}{2}\mathrm{i}\rho \oint_C \langle \overline{W}\rangle^2 \mathrm{d}\bar{z} - 2\mu \oint_C z\frac{\partial\langle\omega\rangle}{\partial z}\mathrm{d}z + \mathrm{i}\rho \oint_C \langle\omega\rangle z\langle \mathrm{d}\Psi\rangle \quad (R\to\infty). \tag{4.10}$$

We note that (4.8), (4.9), and (4.10) are valid in the limit $R\to\infty$, although their correction terms due to ω' are at most $O(R\exp(-kD'R))$ which rapidly converges to zero.

Equation (4.10) implies that the averaged force is described by the mean flow only. The general expression for the force acting on a body in a steady viscous flow has been given by Imai (1951), and is equivalent to (4.10) if we replace the mean components with the corresponding terms for the steady flow. Therefore, applying Imai's result, we obtain:

$$\langle F\rangle = \rho U(\langle m\rangle + \mathrm{i}\langle\Gamma\rangle), \tag{4.11}$$

where $m/2\pi$ and $\Gamma/2\pi$ represent the strength of the source/sink and of the circulation, respectively, for the complex velocity potential $f(z)$ for the region outside the wake:

$$f(z) = Uz + \frac{m+\mathrm{i}\Gamma}{2\pi}\log z - \mathrm{i}\frac{k^{1/2}m^2}{4\pi^{1/2}U}\frac{1}{z^{1/2}} + \left(\frac{\sqrt{3}km^3}{8\pi^2U^2} - \frac{m(m-\mathrm{i}\Gamma)}{2\pi^2U}\right)\frac{\log z}{z} + \frac{a+\mathrm{i}b}{z}\cdots, \tag{4.12}$$

where a and b are constants, and $k=2U/\nu$ (ν is the kinematic viscosity) (Imai 1951). In (4.11), the effect of the flapping motion on the flow is embodied by $\langle m\rangle$ and $\langle\Gamma\rangle$. In particular, $\langle m\rangle$ can be both positive and negative, which is different to the case in which the force acts on a stationary body.

5. Limit of the averaged force acting on the insect for $\langle V\rangle\to 0$

In this section, we present the crux of this paper: the derivation of the paradox. We analyse the forces acting on an insect when the speed of flight is very slow, as in the case of hovering. Supposing that the insect is in a steady state (periodic state) with constant $\langle V\rangle$, the coordinates can be altered such that the time-averaged CM is at the origin.

Taking the x-axis as the direction of the averaged speed and B as the boundary of the wing of the insect, the averaged force $\langle F_x\rangle$ is obtained by:

$$\langle F_x\rangle = -\rho\langle V\rangle\langle m\rangle, \tag{5.1}$$

which is derived from (4.11).

To estimate $\langle m\rangle$, we consider the far-field flow, which is approximated well by the Oseen equation. The general solution of the steady Oseen equation (the temporal average of (3.6)) is:

$$\langle W\rangle(x,y) = e^{kx}\sum_{n=-\infty}^{\infty} C_nK_n(kr)\mathrm{e}^{n\mathrm{i}\theta} + \frac{\mathrm{d}f}{\mathrm{d}z}, \tag{5.2}$$

where C_n are constants, $K_n(kr)$ are modified Bessel functions of the second kind, $r=|z|$, and $f(x,y)=f(z)$ ($z=x+\mathrm{i}y$) is an arbitrary analytic function of z (Imai 1954). Because $f(z)$ is the velocity potential outside the wake, we substitute (4.12) into (5.2) and replace $U=-\langle V\rangle$ and $m=\langle m\rangle$.

The total flux through a circle of extremely large radius is zero owing to the incompressible condition. In complex representation, the flux Q is calculated using

$Q = \mathrm{Im}\left(\oint_C W \mathrm{d}z\right)$, where C is the circle with large radius R. If we denote the first term on the right-hand side of (5.2) as W_{wake}, we obtain

$$\oint_C W_{wake}\mathrm{d}z = \mathrm{i}\sum_{n=-\infty}^{\infty} C_n K_n(kR)R\int_0^{2\pi} \mathrm{e}^{kR\cos\theta}\mathrm{e}^{(n+1)\mathrm{i}\theta}\mathrm{d}\theta \tag{5.3}$$

$$= 2\pi\mathrm{i}R\sum_{n=-\infty}^{\infty} C_n K_n(kR)I_{n+1}(kR), \tag{5.4}$$

where $I_n(kr) \equiv (1/2\pi)\int_0^{2\pi} \mathrm{e}^{kr\cos\theta}\mathrm{e}^{\mathrm{i}n\theta}\mathrm{d}\theta$ is a modified Bessel function of the first kind. Using (4.12) and (5.4), the condition $\lim_{R\to\infty} Q = 0$ reduces to:

$$\sum_{n=-\infty}^{\infty}\frac{\pi}{k}\mathrm{Re}(C_n) + \langle m\rangle = 0, \tag{5.5}$$

where the asymptotic forms $K_n(z) = \sqrt{(\pi/(2z))}\mathrm{e}^{-z}(1 + O(z^{-1}))$ and $I_n(z) = (\mathrm{e}^z/\sqrt{2\pi z})(1 + O(z^{-1}))$ for large $|z|$ are applied.

Let us consider the region where the flow is approximated well by the Oseen equation. In this region, we consider a point P_0 such that its radial coordinate is minimum, and we set the radial coordinate $r = r_0$. In the limit $V \to 0$ ($k \to 0$), kr_0 must converge to zero for the following reason. If $k = 0$, then (3.6) becomes the heat equation, which is isotropic. However, the term $\mathrm{e}^{kx} = \mathrm{e}^{kr\cos\theta}$ in (5.2) introduces an anisotropic effect and hence must vanish as $k \to 0$, which results in $kr_0 \to 0$ as $k \to 0$. In the limit $\langle V\rangle \to 0$ ($kr_0 \to 0$), K_n has the following asymptotic forms:

$$K_0(kr_0) \simeq -\ln\left(\tfrac{1}{2}kr_0\right), \tag{5.6}$$

$$K_n(kr_0) \simeq \tfrac{1}{2}(n-1)!\left(\tfrac{1}{2}kr_0\right)^{-n} \quad (n \geqslant 1). \tag{5.7}$$

Equations (5.6) and (5.7) diverge as $\langle V\rangle \to 0$ ($kr_0 \to 0$).

Applying (5.6) and (5.7) to (5.2), the constant C_n must satisfy the following order for small k:

$$C_0 = O\left(\frac{1}{\ln(kr_0)}\right), \tag{5.8}$$

$$\tfrac{1}{2}C_1\mathrm{e}^{\mathrm{i}\theta} - \frac{\langle m\rangle}{2\pi} = O(kr_0), \tag{5.9}$$

$$C_n = O((kr_0)^n)\ (n \geqslant 2). \tag{5.10}$$

Equations (5.8)–(5.10) and (5.5) lead to:

$$\langle m\rangle = \frac{D_0}{k\ln(kr_0)} + O(kr_0), \tag{5.11}$$

where D_0 is a constant. Using (5.1), (5.5) and (5.11), we obtain:

$$\langle F_x\rangle = 2\rho\nu k\langle m\rangle = \frac{D_0'}{\ln(kr_0)} + O(kr_0), \tag{5.12}$$

where D_0' is a constant independent of kr_0 and $\langle V\rangle$. The limit of (5.12) for $\langle V\rangle \to 0$ is:

$$\lim_{\langle V\rangle\to 0}\langle F_x\rangle = \lim_{kr_0\to 0}\langle F_x\rangle = 0. \tag{5.13}$$

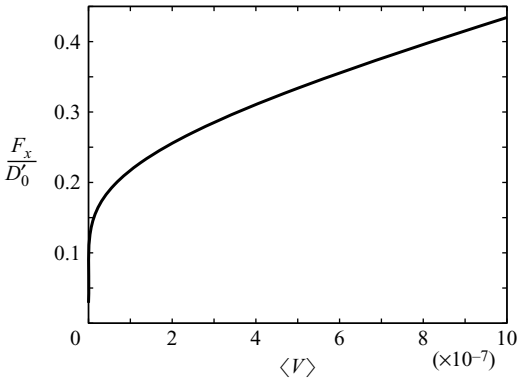

FIGURE 7. Plot of F_x/D_0' for $\nu = 10^{-5}$ and $r_0 = 1$.

We recall that we have assumed a steady flapping flight against an external force: $\boldsymbol{F}_{\text{e.f.}} \cdot \langle \boldsymbol{V} \rangle \neq 0$. Equation (2.2) then gives an expression that allows the flapping motion to be determined:

$$\langle F_x \rangle = -(\boldsymbol{F}_{\text{e.f.}})_x = -\frac{\boldsymbol{F}_{\text{e.f.}} \cdot \langle \boldsymbol{V} \rangle}{|\langle \boldsymbol{V} \rangle|} \neq 0. \tag{5.14}$$

The result (5.13) implies that this equation does not have any solution in the limit $\langle V \rangle \to 0$, regardless of the inclusion of detail concerning the flapping motion. In other words, under the force of gravity, the flapping of the wings of insects should be incapable of generating the net force required for the averaged velocity to be zero.

6. Discussion

The result shown above in (5.13) appears to be paradoxical because real insects appear to hover successfully by flapping their wings. In this section, we examine the validity of the assumptions used in the above calculation and discuss the factors that are important in order for an insect to hover. We evaluate the arguments for and against representing the hovering of a real insect as an exactly stationary state. As will be clarified, the paradox outlined above need not lead to any problems in practice. Nevertheless, the theoretical results presented here describe essential aspects of flapping flight and will be useful for enhancing our knowledge of this type of motion, with the eventual aim of using it in the design of machinery with the capacity to hover.

6.1. *Unsteady hovering*

If it is assumed that a real insect cannot be stationary while hovering, there are two possibilities: $\langle V \rangle \neq 0$ and $\langle V \rangle = 0$.

6.1.1. *The case of* $\langle V \rangle \neq 0$

First, hovering in a practical (biological) sense does not require that $\langle V \rangle$ must be exactly zero. Even if $\langle V \rangle \neq 0$, our theory is able to accommodate the practical sense of hovering because the convergence of the averaged force for $\langle V \rangle \to 0$ is very slow: $F_x = D_0'/\log(2r_0|\langle V \rangle|/\nu)$. In figure 7, a plot of F_x/D_0' is shown for $\nu = 10^{-5}$ ($\text{m}^2\,\text{s}^{-1}$), a typical value for air, and it can be roughly estimated that $r_0 = 1$ [m], which is of the order of a hundred times larger than the size of many insects. In this estimation, the leading term in (5.12) becomes dominant with respect to the second term when

$\langle V \rangle < 10^{-6}$ [m s^{-1}], and the convergence of the averaged force is slow even for this range.

A practical definition of hovering is $J \equiv \langle V \rangle T/(2l_s) < 0.1$, where l_s is the sweeping length of the flapping (J is the advance ratio; see Dudley 2000). Even for butterflies, for which there is a strict range limitation $\langle V \rangle$ owing to the long flapping period, this definition implies that they achieve hovering when $\langle V \rangle$ is less than the order of 10^{-2} [m s^{-1}], according to the estimation that $T = 10^{-1}$ [s] and $l_s = 10^{-2}$ [m].

Therefore, such force reduction takes place over a limited range of velocities. However, discussing this limitation will be useful in order to understand that critical behaviour can occur as $\langle V \rangle \to 0$. For example, numerical simulation yields an N-shaped curve for the hydrodynamic force generated by a horizontally flapping wing as a function of the speed of a vertical uniform flow (Iima 2007). This N-shape can be interpreted as representing a smoothing-out of the singularity owing to the limitations that are intrinsic to the numerical simulation, although a detailed comparison should be performed (in the simulation, a non-periodic flow is observed when $\langle V \rangle = 0$; see also section 6.1.2).

This problem would become more serious when developing a flapping-flight machine that can hover for an extended period of time. The above estimate ($\langle V \rangle \sim 10^{-6}$ [m s^{-1}]) gives a one-day ($\sim 10^5$ [s]) increment in position of the order of 0.1 [m]. This strategy would be appropriate for such a machine to achieve hovering if it were able to sustain its weight under the force reduction due to the small $\langle V \rangle$. However, this would require a control system enabling the machine to return to its original position by non-periodic wing motion, which is outside the scope of the present theory.

6.1.2. *The case of* $\langle V \rangle = 0$

One strategy that can be used to explain how hovering is achieved involves the unsteady effect. This strategy may be followed using two different methods: the first uses the unsteady term $-(\mathrm{d}/\mathrm{d}t)\mathscr{P}$ while the other uses the concept of non-periodicity.

The unsteady term $-(\mathrm{d}/\mathrm{d}t)\mathscr{P}$ in (4.1) does not affect the period-averaged force if the flow is temporally periodic; however, if we consider unsteady and non-periodic motion, this term generates hydrodynamic force. The following simple model might be useful for illustrating this strategy. We first suppose that a wing is flapping horizontally in a temporally periodic manner, making an inverted Kármán vortex street that is observed during normal hovering (figure 8). We then imagine that the flapping motion has been occurring for a finite time. In this case, the region of non-zero vorticity is bounded, while a complex velocity potential exists outside this region. The motion of the wing is assumed to be time-periodic, but the length of the vortex arrays is assumed to be elongated by the flapping. In the simplest case, we assume the vortex field to be comprised of two vertical vortex sheets of finite length $l(t)$ and with a strength of $\pm\kappa$. The complex potential $f(z)$ of the induced flow is:

$$f(z) = -\int_{-l}^{0} \mathrm{i}\kappa \log \frac{z-(a+\mathrm{i}y)}{z-(-a+\mathrm{i}y)}\mathrm{d}y. \tag{6.1}$$

In the far field ($|z| \gg l$), $f(z)$ and W take the following forms:

$$f(z) \simeq \frac{2\mathrm{i}\kappa a l}{z}, \quad W = \frac{\mathrm{d}f}{\mathrm{d}z} = -\frac{2\mathrm{i}\kappa a l}{z^2}. \tag{6.2}$$

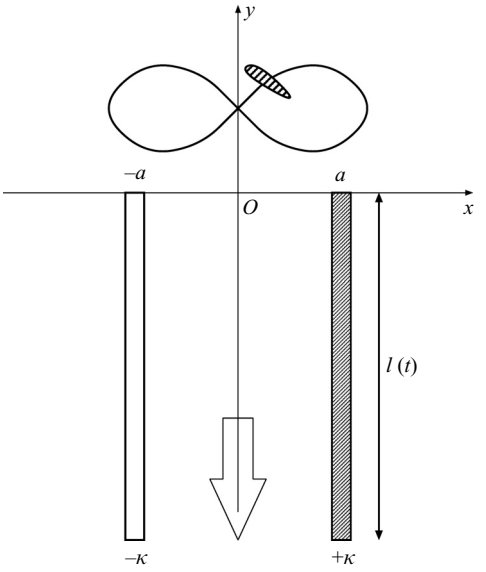

FIGURE 8. A hovering model for which the finite-time effect is considered. Wing flapping generates an inverted Kármán street, which is simplified to a pair of vortex sheets of finite length $l(t)$ along the y-direction. The strength for unit length is $-\kappa$ (left) and $+\kappa$ (right); positive and negative signs are denoted by grey and white, respectively. Note that the actual thickness of each vortex sheet is zero, although the diagram uses a finite thickness to indicate the sign of the strength. The induced flow between the vortex sheets is downward, which generates hydrodynamic force.

Using (4.2) and (4.3) by taking C to be a large circle, we then obtain:

$$F_0 = 0, \tag{6.3}$$

$$\mathscr{P} = 4\pi \mathrm{i}\rho\kappa a l(t) - \rho \oint_B z \mathrm{d}\Psi. \tag{6.4}$$

It should be noted that this simplified model is used merely to illustrate the idea. For a general vorticity distribution, only the term proportional to z^{-1}, the dipole term, contributes to the integral. The only difference is the value of the coefficient. The period-averaged hydrodynamic force for this model is:

$$F = 4\pi \mathrm{i}\rho\kappa a V, \quad V = \frac{l(t+T) - l(t)}{T}. \tag{6.5}$$

We note that the second term in (6.4) drops out owing to the periodicity. This example illustrates the generation of an unsteady force by the time derivative of $\mathscr{P}$. The definition of $\mathscr{P}$ actually includes the hydrodynamic impulse as the first term in (A 36). However, this effect vanishes when $\mathscr{P}$ converges to a temporally periodic function.

To understand the relationship between the assumption of periodicity and the other assumptions involved in the calculation, it is necessary to consider what happens to the flow field if a non-zero averaged force is generated when $\langle V \rangle = 0$. In this case, the elliptical regions $\mathscr{A}_n$ $(n > 0)$ are still bounded (§ 3.2), but the parabolic regions $\mathscr{A}_0$ cover the entire space, which means that the derivation in §§ 4 and 5 is not valid. Therefore, this scenario requires separate discussion.

When $\langle V\rangle = 0$, a velocity scale is required in order to evaluate the order of the nonlinear term. To do this, we rewrite (2.5) using T, $\sqrt{\nu T}$ and U_0 as typical values of time, length and velocity, respectively:

$$\frac{\partial\tilde{\omega}}{\partial\tilde{t}} - \tilde{\Delta}\tilde{\omega} = \chi\frac{\partial(\tilde{\Psi},\tilde{\omega})}{\partial(\tilde{x},\tilde{y})}, \tag{6.6}$$

where $\tilde{*}$ are dimensionless variables and $\chi \equiv U_0\sqrt{T/\nu}$. Because we assume that $\lim_{|r|\to\infty}\boldsymbol{u} = 0$, the far field may be defined by the region outside the circle such that $\chi \ll 1$ when U_0 is the maximum velocity in the region. Equation (6.6) shows that the flow in the far field is governed by the Stokes equation as a first approximation. We note that the discussion is similar to that in § 3.1 when $n \neq 0$, because $s_n \neq 0$. However, the modes $n = 0$ must be treated separately because $s_n = 0$. When $n \neq 0$, a similar discussion leads to the result that $|\omega_{m,n}| \leqslant C_{max}r^{-1/2}\exp(-\alpha_n r)$: the wake region $\mathscr{A}_n$ is also bounded even if $\langle V\rangle = 0$. Thus, we need only consider the mean flow. According to the theory of two-dimensional steady Stokes flow by Imai (1972), the far-field flow can be described using two analytic functions $g(z)$ and $h(z)$ as follows:

$$W = \overline{z}\frac{\mathrm{d}g}{\mathrm{d}z} - \overline{g(z)} + \frac{\mathrm{d}h}{\mathrm{d}z},\ \omega = -4\mathrm{Im}\left(\frac{\mathrm{d}g}{\mathrm{d}z}\right), \tag{6.7a,b}$$

where

$$g(z) = -c\log z + \sum_{n=-\infty}^{\infty} D_n z^n, \tag{6.8}$$

$$h(z) = \overline{c}(z\log z - z) + (m + \mathrm{i}\kappa)\log z + \sum_{n=-\infty}^{\infty} C_n z^n, \tag{6.9}$$

where c, C_n and D_n are constants. Because $\langle V\rangle = 0$, we impose the condition that $\lim_{z\to\infty} W = 0$, which leads to:

$$c = 0, \quad C_n = 0\ (n > 0), \quad D_n = 0\ (n > 0). \tag{6.10}$$

Equation (6.7b) shows that the vorticity decays as a power of r, which is different to the case in which $\langle V\rangle \neq 0$. In this sense, the wake covers the entire space. To evaluate the force acting on the wing, it is convenient to use the following form of the force formula (4.1):

$$F = \left\{-\mathrm{i}\oint_C p\,\mathrm{d}\overline{z} + 4\mu\oint_C \frac{\partial^2\Psi}{\partial\overline{z}^2}\mathrm{d}\overline{z}\right\} - \rho\oint_C \overline{W}\mathrm{Im}(W\,\mathrm{d}z) - \frac{\mathrm{d}P_0}{\mathrm{d}t}, \tag{6.11}$$

which is easily derived using (A 18). P_0 is defined in (A 26). The first two terms (in brackets) in (6.11) are the same as those employed in the force formula for steady Stokes flow (Imai 1972). The third term may be neglected owing to the low velocity, and even if it is calculated, it vanishes because $W = O(z^{-1})$. The fourth term in (6.11) vanishes owing to the period averaging. Therefore,

$$\langle F\rangle = 8\pi\mu c = 0. \tag{6.12}$$

We hence obtain the same result, that $\langle F\rangle = 0$ if $\langle V\rangle = 0$. The coefficient c is related to the strength of the two-dimensional Stokeslet (Imai 1972), which causes divergence of the flow at infinity. Therefore, our assumption that the flow should converge to become uniform excludes the possibility of the existence of a two-dimensional Stokeslet as the source of the force. This reminds us of the Stokes paradox, that there

is no solution to the Stokes equation for the translation of a cylinder with constant velocity through an infinite mass of liquid (Lamb 1997, § 343). In the present paradox, the Stokes paradox is extended to take periodic flow into account, and the conclusion of the Stokes paradox corresponds to the zero averaged force for a hovering insect.

Another possible way of explaining hovering is to assume that the periodicity is not actually satisfied. Even if the flapping motion is temporally periodic, the flow can be non-periodic. This can be the case even when the Reynolds number is of the order of 10 (Blondeaux & Guglielmini 2005). The experimental study of flapping wings under uniform flows has shown that the vortex street generated by a flapping wing exhibits a deflection. The deflection angle varies in a non-periodic manner when the speed of the uniform flow is small (Knoller-Betz effect; Jones, Dohring & Platzer 1998). Measurements of induced flow for a tethered hawkmoth suggests some non-periodicity (Sane & Jacobson 2006). These observations suggest that non-periodicity occurs when $\langle V \rangle$ is small. If we regard the non-periodic flow as the limit of the periodic flow as $T \to \infty$, then the wake region of the fluctuation component $\mathscr{A}_1$ covers the whole space because $\lim_{T\to\infty} l_1 = \infty$. In this case, the net force depends on the fluctuation component of the flow. Such fluctuation will occur when the Reynolds number is large enough to cause instability in the flow. Another factor that might give rise to fluctuation is that insects can change the amplitude of flapping to break the periodicity of the flow, which implies that an active control method is necessary to achieve hovering flight.

6.2. *Steady hovering*

We now consider the scenario in which real insects achieve hovering even if the flow is temporally periodic and $\langle V \rangle = 0$ in the exact sense. In this case, the limitations of two-dimensional treatments should be considered. The proof is based on the assumption that the flow in the far field is decomposed into a potential velocity and a wake velocity. This assumption is valid for two-dimensional flow with general Reynolds numbers. However, for three-dimensional flow it is not generally valid (Chadwick 1998) and in this case the flow in the far field should be carefully calculated; this will be considered elsewhere.

7. Concluding remarks

We have presented the paradox that a hovering insect cannot generate non-zero averaged force in two-dimensional space if the induced flow is temporally periodic. With the help of a generalized Blasius formula (Imai 1974), the averaged force acting on a periodically oscillating body can be evaluated solely in terms of the far field time-averaged flow. We have shown that the averaged force acting on the insect becomes zero as $\langle V \rangle \to 0$, where $\langle V \rangle$ is the averaged velocity of the insect. This suggests that the periodic flapping motion does not generate a non-zero net force.

The derivation of this paradox demonstrates that the fluctuation component of the far field for any temporally periodic flow is confined to a finite region. This fact enables us to evaluate the averaged force in the same way as the force acting on a stationary body, except for the sign of $\langle m \rangle$.

Several problems that occur in a near-hovering state are revealed by this paradox; to achieve hovering, at least one of our assumptions must be broken. The assumption of periodicity may be related to the importance of some control system. As discussed in § 6, non-periodic flow will actually lead to the generation of hydrodynamic force during hovering. Real insects may control the flapping of their wings during hovering

not only to stabilize their state, but also to generate hydrodynamic force. Boundary effects may also be important. If the ground or a wall is in close proximity, that is, if the region occupied by the fluid is not large enough to apply the far-field approximation, some measurements will depend on the properties of the boundary. Convergence of the flow to uniformity appears to be a reasonable assumption, but we have shown that this assumption leads to a similar conclusion to the Stokes paradox.

The relationship between this paradox and real insects should, however, be considered carefully. The convergence 'speed' $1/\log(|\langle V\rangle|)$ is so slow that reduction of the force may not be a practical problem for real insects. Nevertheless, this paradox is interesting from a theoretical viewpoint, and may provide important insight that could eventually be applied to the development of a flying machine that can hover for a long period of time. In this paper, we have used properties of the far field flow to evaluate the hydrodynamic force of flapping-flight; our method is suited to treating this kind of problem because the far field is governed by the Oseen equation, a linear equation, and its qualitative characteristics do not depend on details of the flapping motion. An analogy may be drawn with the Kutta–Jowkowski theorem, in which only two properties of the far-field flow of the wing, the circulation of the wing and the uniform flow, determine the lift. For a more quantitative calculation of a particular type of wing motion, more detailed information on the far-field flow induced by the wing motion is required. In the case of three-dimensional steady flow, Chadwick & Fishwick (2007) have proposed a theory of lift based on the Oseen model. An extension of this method is under development, and details will be published elsewhere. It is expected that this result will improve our understanding of the forces acting on a body in a fluid.

The author would like to thank Professor K. Ohkitani for discussions and Professor Y. Miyamoto for reading a draft of this paper. This research was partially supported by a Grant-in-Aid for Young Scientists (B), 2007–2008, 19740228, and Scientific Research on Priority Areas, 2008–2009, 20033009 from the Ministry of Education, Science, Sports and Culture of Japan.

Appendix. A proof of Imai's formula

Imai (1974) derived formulae for the force and moment acting on a moving body in both two- and three-dimensional space. These formulae are generalized force formulae derived from the Navier–Stokes equations without approximation. However, the only existing literature concerning the formulae consists of a conference abstract, written in Japanese, in which no proof is given. Proof of the force formula for two-dimensional space is therefore provided here.

A.1. *Preparation*

For a vector field in two-dimensional space, $\boldsymbol{A} = (A_x(x, y), A_y(x, y))$ (where A_x and A_y are real-valued functions of x and y), we consider a complex variable in the complex plane $A(z, \bar{z}) \equiv A_x + \mathrm{i}A_y$ ($\mathrm{i} = \sqrt{-1}$), where $z = x + \mathrm{i}y$. In this paper, we refer to this complex variable as the complex representation of $\boldsymbol{A}$. This relation will hereinafter be denoted as $\boldsymbol{A} \mapsto A$.

A simple example is:

$$\frac{\partial A}{\partial z} = \tfrac{1}{2}\{(\nabla \cdot \boldsymbol{A}) + \mathrm{i}(\nabla \times \boldsymbol{A}) \cdot \boldsymbol{e}_z\} \ (\boldsymbol{e}_z \text{ is a unit vector in the } z\text{-axis}). \qquad (A\,1)$$

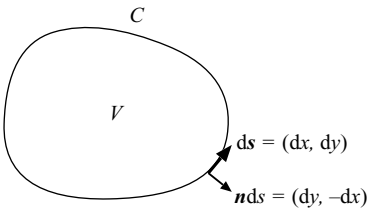

FIGURE 9. Schematic picture of the volume V bounded by C and the line element.

Several formulae for a vector field can be rewritten in the form of a complex representation. Let us define the line element $\mathrm{d}\boldsymbol{s}$ as in figure 9, and $\boldsymbol{n}$ as a unit vector on C whose direction is outside the boundary.

If A is a complex-valued function of $(z, \bar{z})$, the integral of $\partial A/\partial z$ over the volume V bounded by C is given by:

$$\int_V \frac{\partial}{\partial z} A \mathrm{d}V = \tfrac{1}{2}\mathrm{i} \oint_C A \mathrm{d}\bar{z}, \quad \int_V \frac{\partial}{\partial \bar{z}} \overline{A} \mathrm{d}V = -\tfrac{1}{2}\mathrm{i} \oint_C \overline{A} \mathrm{d}z \tag{A 2}$$

(Milne-Thomson 1968). The proofs of (A 2) are simple if the formulae are rewritten in Cartesian coordinates and the Gauss and Stokes theorems are applied. The complex velocity W is defined as $W = u - \mathrm{i}v$, where $\boldsymbol{u} = (u, v)$ is the flow field. Substituting W into (A 1) and taking the complex conjugate gives:

$$\frac{\partial W}{\partial \bar{z}} = \tfrac{1}{2}\{(\nabla \cdot \boldsymbol{u}) - \mathrm{i}(\nabla \times \boldsymbol{u}) \cdot \boldsymbol{e}_z\}. \tag{A 3}$$

In particular, if the flow is incompressible ($\nabla \cdot \boldsymbol{u} = 0$) and irrotational ($\nabla \times \boldsymbol{u} = 0$), then: $\partial_{\bar{z}} W = 0$. Because the condition $\partial_{\bar{z}} W = 0$ is equivalent to the Cauchy–Riemann relation, W is an analytic function of z. Using the complex potential $f(z)$, we obtain the relationship between W and f as:

$$W = \frac{\mathrm{d}f}{\mathrm{d}z}. \tag{A 4}$$

If the flow is rotational ($\nabla \times \boldsymbol{u} \neq 0$), then W is a function of $(z, \bar{z})$. Hereinafter, the flow is assumed to be incompressible such that $\mathrm{Re}(\partial W/\partial \bar{z}) = 1/2 \nabla \cdot \boldsymbol{u} = 0$, but rotational in general.

By using the streamfunction Ψ such that $(u, v) = (\partial \Psi/\partial y, -\partial \Psi/\partial x)$ (equation (2.6)), we obtain the following relations:

$$W = 2\mathrm{i}\frac{\partial \Psi}{\partial z}, \quad \omega = -2\mathrm{i}\frac{\partial \overline{W}}{\partial z} = -4\frac{\partial^2 \Psi}{\partial z \partial \bar{z}}, \tag{A 5}$$

where $\omega \equiv (\nabla \times \boldsymbol{u}) \cdot \boldsymbol{e}_z$ is the vorticity. We define the total pressure Q by $Q = p/\rho + 1/2q^2/2$, where $q^2 \equiv u^2 + v^2 = W\overline{W}$ (p is the pressure and ρ is the density).

Using these relations, the Navier–Stokes equations ((2.3) and (2.4)) can be described by:

$$\mathrm{i}\frac{\partial}{\partial t}\frac{\partial \Psi}{\partial z} + \frac{\partial Q}{\partial z} + \omega \frac{\partial \Psi}{\partial z} + \mathrm{i}\nu \frac{\partial \omega}{\partial z} = 0, \tag{A 6}$$

where ν is the kinematic viscosity (see Imai (1951) for the steady analogue of (A 6)).

A.2. *Proof*

We consider a body of arbitrary deformable shape moving in a fluid, where B, C and S are the boundary of the body, the boundary of the control volume that includes

B, and the volume bounded by B and C, respectively (see figure 6). We assume that B depends on time, but that C does not depend on time. The integration of the Navier–Stokes equation (2.3) over the volume S gives:

$$\int_B \boldsymbol{\sigma}_n \mathrm{d}s + \int_C \boldsymbol{\sigma}_n \mathrm{d}s + \iint_S \left(\boldsymbol{K} - \rho \frac{\mathrm{D}\boldsymbol{u}}{\mathrm{D}t} \right) \mathrm{d}V = 0, \tag{A 7}$$

where $\boldsymbol{K}$ is an external force, $\mathrm{D}/\mathrm{D}t = \partial/\partial t + (\boldsymbol{u} \cdot \nabla)$ is the Lagrange derivative, $\boldsymbol{u}$ is the velocity, $\boldsymbol{\sigma}_n = \boldsymbol{\sigma} \cdot \boldsymbol{n}$, $\boldsymbol{n}$ is the normal unit vector on the boundary, and $\boldsymbol{\sigma}$ is the stress tensor. The component of the stress tensor is:

$$\sigma_{ij} = -p\delta_{ij} + 2\mu e_{ij}, \quad e_{ij} = \frac{1}{2}\left(\frac{\partial u_i}{\partial x_j} + \frac{\partial u_j}{\partial x_i} \right), \tag{A 8}$$

where e_{ij} is the component of the deformation rate tensor ($u_x = u, u_y = v$), $\boldsymbol{e}$, and $\mu \equiv \rho\nu$ is the viscosity coefficient. We assume that an external force $\boldsymbol{K}$ has a potential, and that $\boldsymbol{K}$ can be included in the pressure.

Equation (A 7) is equivalent to:

$$\int_B (\boldsymbol{\sigma}_n - \rho \boldsymbol{u} u_n)\mathrm{d}s + \int_C (\boldsymbol{\sigma}_n - \rho \boldsymbol{u} u_n)\mathrm{d}s + \iint_S \left(-\rho \frac{\partial \boldsymbol{u}}{\partial t} \right) \mathrm{d}V = 0 \ (u_n \equiv \boldsymbol{u} \cdot \boldsymbol{n}). \tag{A 9}$$

Because the force acting on B, $\boldsymbol{F}$, is $\boldsymbol{F} = -\int_B \boldsymbol{\sigma}_n \mathrm{d}s$, we obtain:

$$\boldsymbol{F} = \boldsymbol{F}_1 + \boldsymbol{F}_2, \tag{A 10}$$

$$\boldsymbol{F}_1 = \int_C (\boldsymbol{\sigma}_n - \rho \boldsymbol{u} u_n)\mathrm{d}s, \tag{A 11}$$

$$\boldsymbol{F}_2 = -\left(\int_B \rho \boldsymbol{u} u_n \mathrm{d}s + \rho \iint_S \frac{\partial \boldsymbol{u}}{\partial t} \mathrm{d}V \right). \tag{A 12}$$

Equations (A 10)–(A 12) can be described using complex forms as follows.

First, we show that:

$$\boldsymbol{\sigma}_n \mathrm{d}s \mapsto \mathrm{i}p\mathrm{d}z + 4\mu \frac{\partial^2 \Psi}{\partial \bar{z}^2} \mathrm{d}\bar{z}, \tag{A 13}$$

which can easily be checked using the relations:

$$-p\boldsymbol{n}\mathrm{d}s \mapsto \mathrm{i}p\mathrm{d}z, \quad \boldsymbol{e} \cdot \boldsymbol{n}\mathrm{d}s \mapsto 2\frac{\partial^2 \Psi}{\partial \bar{z}^2}\mathrm{d}\bar{z}. \tag{A 14}$$

Next,

$$u_n \mathrm{d}s \mapsto \mathrm{Im}(W\mathrm{d}z) \left(= \frac{\partial \Psi}{\partial z}\mathrm{d}z + \frac{\partial \Psi}{\partial \bar{z}}\mathrm{d}\bar{z} = \mathrm{d}\Psi \right). \tag{A 15}$$

This leads to

$$-\rho \boldsymbol{u} u_n \mathrm{d}s \mapsto -\rho \overline{W} \mathrm{Im}(W\mathrm{d}z). \tag{A 16}$$

Thus, we obtain F_1 ($\boldsymbol{F}_1 \mapsto F_1$) as:

$$F_1 = \oint_C \mathrm{d}F_1, \tag{A 17}$$

$$\mathrm{d}F_1 = \mathrm{i}p\mathrm{d}z + 4\mu \frac{\partial^2 \Psi}{\partial \bar{z}^2}\mathrm{d}\bar{z} - \rho \overline{W} \mathrm{Im}(W\mathrm{d}z). \tag{A 18}$$

The integral element $\mathrm{d}F_1$ is rewritten as

$$\mathrm{d}F_1 = -\tfrac{1}{2}\mathrm{i}\rho\overline{W}^2\mathrm{d}\bar{z} + \mathrm{d}\left(\mathrm{i}\rho Qz + 4\mu\frac{\partial\Psi}{\partial\bar{z}} + \mu\omega z\right) - 2\mu z\frac{\partial\omega}{\partial z}\mathrm{d}z + \mathrm{i}\rho z\frac{\partial}{\partial t}\{\mathrm{Re}(W\mathrm{d}z)\} + \mathrm{i}\rho\omega z\mathrm{d}\Psi, \quad \text{(A 19)}$$

by using the following relations:

$$\mathrm{i}p\mathrm{d}z - \rho\overline{W}\mathrm{Im}(W\mathrm{d}z) = \mathrm{i}\rho Q\mathrm{d}z - \frac{1}{2}\mathrm{i}\rho\overline{W}^2\mathrm{d}\bar{z}, \quad \text{(A 20)}$$

$$\mathrm{d}Q = -\frac{\partial}{\partial t}\{\mathrm{Re}(W\mathrm{d}z)\} - \omega\mathrm{d}\Psi + 2\nu\mathrm{Im}\left(\frac{\partial\omega}{\partial z}\mathrm{d}z\right), \quad \text{(A 21)}$$

$$\mathrm{d}\left(\frac{\partial\Psi}{\partial\bar{z}}\right) = \frac{\partial}{\partial\bar{z}}\mathrm{d}\Psi = -\tfrac{1}{4}\omega\mathrm{d}z + \frac{\partial^2\Psi}{\partial\bar{z}^2}\mathrm{d}\bar{z}. \quad \text{(A 22)}$$

Finally, by using (A 17) and (A 19), F_1 is expressed as follows:

$$F_1 = \oint_C \mathrm{d}F_1 \quad \text{(A 23)}$$

$$= -\tfrac{1}{2}\mathrm{i}\rho\oint_C \overline{W}^2\mathrm{d}\bar{z} - 2\mu\oint_C z\frac{\partial\omega}{\partial z}\mathrm{d}z + \mathrm{i}\rho\oint_C \omega z\mathrm{d}\Psi + \mathrm{i}\rho\oint_C z\frac{\partial}{\partial t}\{\mathrm{Re}(W\mathrm{d}z)\}. \quad \text{(A 24)}$$

We now derive the complex form of $\boldsymbol{F}_2$. It is easy to show that:

$$\boldsymbol{F}_2 = -\frac{\mathrm{d}\boldsymbol{P}_0}{\mathrm{d}t}, \quad \boldsymbol{P}_0 = \rho\iint_S \boldsymbol{u}\mathrm{d}V. \quad \text{(A 25)}$$

The complex representation of $\boldsymbol{P}_0$, $P_0 = \rho\int_S \overline{W}\mathrm{d}V$, is expressed in the following two ways:

$$P_0 = \rho\oint_{B+C} z\mathrm{d}\Psi, \quad \text{(A 26)}$$

$$P_0 = -\mathrm{i}\rho\int_S z\omega\mathrm{d}V + \tfrac{1}{2}\mathrm{i}\rho\oint_{B+C} z(\overline{W}\mathrm{d}\bar{z} + W\mathrm{d}z). \quad \text{(A 27)}$$

Equations (A 26) and (A 27) are obtained as follows. We substitute $A = z\overline{W}$ and $\overline{A} = zW$ into (A 2) to obtain:

$$\int_S \overline{W}\mathrm{d}V + \tfrac{1}{2}\mathrm{i}\int_S z\omega\mathrm{d}V = \tfrac{1}{2}\mathrm{i}\oint_{B+C} z\overline{W}\mathrm{d}\bar{z}, \quad -\tfrac{1}{2}\mathrm{i}\int_S z\omega\mathrm{d}V = -\tfrac{1}{2}\mathrm{i}\oint_{B+C} zW\mathrm{d}z. \quad \text{(A 28)}$$

The sum of the two equations gives:

$$\int_S \overline{W}\mathrm{d}V = \tfrac{1}{2}\mathrm{i}\oint_{B+C} z(\overline{W}\mathrm{d}\bar{z} - W\mathrm{d}z) = \oint_{B+C} z\mathrm{d}\Psi. \quad \text{(A 29)}$$

The difference of the two relations gives:

$$\int_S \overline{W}\mathrm{d}V + \mathrm{i}\int_S z\omega\mathrm{d}V = \tfrac{1}{2}\mathrm{i}\oint_{B+C} z(\overline{W}\mathrm{d}\bar{z} + W\mathrm{d}z). \quad \text{(A 30)}$$

By using the identities (A 29) and (A 30), we can prove that (A 26) and (A 27), respectively.

We now calculate the time derivative of P_0. Equation (A 26) leads to:

$$\frac{\mathrm{d}P_0}{\mathrm{d}t} = \frac{\mathrm{d}}{\mathrm{d}t}\left\{\rho \oint_C z\mathrm{d}\Psi\right\} - \frac{\mathrm{d}}{\mathrm{d}t}\left\{\rho \oint_B z\mathrm{d}\Psi\right\}$$
$$= \mathrm{i}\rho \oint_C z\frac{\partial}{\partial t}\{\mathrm{Re}(W\mathrm{d}z)\} - \frac{\mathrm{d}}{\mathrm{d}t}\left\{\mathrm{i}\rho \oint_C zW\mathrm{d}z + \rho \oint_B z\mathrm{d}\Psi\right\} \quad (A\,31)$$

by using the relation $z\mathrm{d}\Psi = \mathrm{i}z\mathrm{Re}(W\mathrm{d}z) - \mathrm{i}zW\mathrm{d}z$ (note that C is time-independent).

Equation (A 27) leads to:

$$\frac{\mathrm{d}P_0}{\mathrm{d}t} = \frac{\mathrm{d}}{\mathrm{d}t}\left\{-\mathrm{i}\rho \int_S z\omega\mathrm{d}V - \tfrac{1}{2}\mathrm{i}\rho \oint_B z(\overline{W}\mathrm{d}\overline{z} + W\mathrm{d}z)\right\} + \mathrm{i}\rho \oint_C z\frac{\partial}{\partial t}(\mathrm{Re}(W\mathrm{d}z)). \quad (A\,32)$$

In summary, we have two expressions for F_2:

$$F_2 = \frac{\mathrm{d}}{\mathrm{d}t}\left\{\mathrm{i}\rho \oint_C zW\mathrm{d}z + \rho \oint_B z\mathrm{d}\Psi\right\} - \mathrm{i}\rho \oint_C z\frac{\partial}{\partial t}\{\mathrm{Re}(W\mathrm{d}z)\}, \quad (A\,33)$$

$$F_2 = \frac{\mathrm{d}}{\mathrm{d}t}\left\{\mathrm{i}\rho \int_V z\omega\mathrm{d}V + \tfrac{1}{2}\mathrm{i}\rho \oint_B z(\overline{W}\mathrm{d}\overline{z} + W\mathrm{d}z)\right\} - \mathrm{i}\rho \oint_C z\frac{\partial}{\partial t}(\mathrm{Re}(W\mathrm{d}z)). \quad (A\,34)$$

The final expression for $F = F_1 + F_2$ is now:

$$F = -\tfrac{1}{2}\mathrm{i}\rho \oint_C \overline{W}^2\mathrm{d}\overline{z} - 2\mu \oint_C z\frac{\partial\omega}{\partial z}\mathrm{d}z + \mathrm{i}\rho \oint_C \omega z\mathrm{d}\Psi - \frac{\mathrm{d}}{\mathrm{d}t}\mathscr{P}, \quad (A\,35)$$

where

$$\mathscr{P} = -\mathrm{i}\rho \int_S z\omega\mathrm{d}V - \tfrac{1}{2}\mathrm{i}\rho \oint_B z(\overline{W}\mathrm{d}\overline{z} + W\mathrm{d}z), \quad (A\,36)$$

or

$$\mathscr{P} = -\mathrm{i}\rho \oint_C zW\mathrm{d}z - \rho \oint_B z\mathrm{d}\Psi. \quad (A\,37)$$

Equations (A 35)–(A 37) comprise Imai's force formula, first derived by Imai (1974). If the flow is steady and irrotational such that $\omega = 0$, $\mathrm{d}/\mathrm{d}t = 0$, we obtain the Blasius formula: $F = -4(\mathrm{i}/2)\rho \oint_C \overline{W}^2\mathrm{d}\overline{z}$. The first term on the right-hand side of (A 36) is the hydrodynamic impulse in the two-dimensional case.

REFERENCES

Betts, C. R. & Wootton, R. J. 1988 Wing shape and flight behaviour in butterflies (*Lepidoptera: Papilionoidea* and *Hesperioidea*): a preliminary analysis. *J. Expl Biol.* **138**, 271–288.

Blondeaux, P. & Guglielmini, L. 2005 Chaotic flow generated by an oscillating foil. *AIAA J.* **43**, 918–922.

Chadwick, E. 1998 The far-field Oseen velocity expansion. *Proc. R. Soc. Lond.* A **454**, 2059–2082.

Chadwick, E. & Fishwick, N. 2007 Lift on slender bodies with elliptical cross section evaluated by using an Oseen flow model. *SIAM J. Appl. Maths.* **67**, 1465–1478.

Childress, S. 1981 *Mechanics of Swimming and Flying*. Cambridge University Press.

Childress, S., Vandenberghe, N. & Zhang, J. 2006 Hovering of a passive body in an oscillating airflow. *Phys. Fluids* **18**, 117103.

Dickinson, M. H. & Götz, K. G. 1993 Unsteady aerodynamic performance of model wings at low Reynolds numbers. *J. Expl Biol.* **174**, 45–64.

Dickinson, M. H., Lehmann, F.-O. & Sane, S. P. 1999 Wing rotation and the aerodynamic basis of insect flight. *Science* **284**, 1954–1960.

Dudley, R. 2000 *The Biomechanics of Insect Flight*. Princeton University Press.

Edwards, R. H. & Cheng, H. K. 1982 The separation vortex in the Weis-Fogh circulation-generation mechanism. *J. Fluid Mech.* **120**, 463–473.

Ellington, C. P. 1984 The aerodynamics of hovering insect flight. *Phil. Trans. R. Soc. Lond.*B **305**, 1–180.

Ellington, C. P., Berg, C., Willmott, A. P. & Thomas, A. L. R. 1996 Leading-edge vortices in insect flight. *Nature* **384**, 626–630.

Iima, M. 2007 A two-dimensional aerodynamic model of freely flying insects. *J. Theor. Biol.* **247**, 657–671.

Iima, M. & Yanagita, T. 2001*a* An analysis of a symmetric flapping model: a symmetry-breaking mechanism and its universality. *Theor. Appl. Mech.* **50**, 237–245.

Iima, M. & Yanagita, T. 2001*b* Is a two-dimensional butterfly able to fly by symmetric flapping? *J. Phys. Soc. Japan* **70**, 5–8.

Iima, M. & Yanagita, T. 2005 Asymmetric motion of a two-dimensional symmetric flapping model. *Fluid Dyn. Res.* **36**, 407–425.

Iima, M. & Yanagita, T. 2006 A transition of ascending flight to vertical hovering: a study of a symmetric flapping model. *Europhys. Lett.* **74**, 55–61.

Imai, I. 1951 On the asymptotic behaviour of viscous fluid flow at a great distance from a cylindrical body, with special reference to Filon's paradox. *Proc. R. Soc. Lond.* A **208**, 487–516.

Imai, I. 1954 A new method of solving Oseen's equations and its application to the flow past an inclined elliptic cylinder. *Proc. R. Soc. Lond.* A **224**, 141–160.

Imai, I. 1972 Some applications of function theory to fluid dynamics. In *The Second International JSME Symp. Fluid Machinery and Fluidics, Tokyo*, pp. 15–23.

Imai, I. 1974 Kasou shitsuryou to kasou undouryou–uzu undou he no ouyou (virtual mass and virtual angular momentum – an application to vortex motion; in Japanese). *Abstr. Meeting of the Phys. Soc. Japan. Annual Meeting* **29**, 14–16.

Jones, K. D., Dohring, C. M. & Platzer, M. F. 1998 Experimental and computational investigation of the Knoller–Betz effect. *AIAA J.* **36**, 1240–1246.

Lamb, H. 1997 *Hydrodynamics,* 6th ed., Cambridge University Press.

Liu, H., Ellington, C. P., Kawachi, K., Berg, C. V. D. & Willmott, A. P. 1998 A computational fluid dynamic study of hawkmoth hovering. *J. Expl Biol.* **201**, 461–477.

Maxworthy, T. 1979 Experiments on the Weis-Fogh mechanism of lift generation by insects in hovering flight. Part 1. Dynamics of the 'fling'. *J. Fluid. Mech.* **93**, 47–63.

Milne-Thomson, L. M. 1968 *Theoretical Hydrodynamics* 5th edn., Dover.

Noca, F., Shiels, D. & Jeon, D. 1997 Measuring instantaneous fluid dynamic forces on bodies, using only velocity fields and their derivatives. *J. Fluids Struct.* **11**, 345–350.

Pesavento, U. & Wang, Z. J. 2004 Falling paper: Navier–Stokes solutions, model of fluid forces, and center of mass elevation. *Phys. Rev. Lett.* **93**, 144501.

Riley, N. 1967 Oscillatory viscous flows. Review and extension. *J. Inst. Maths Applics.* **3**, 419–434.

Sane, S. P. & Dickinson, M. H. 2002 The aerodynamic effects of wing rotation and a revised quasi-steady model of flapping flight. *J. Expl Biol.* **205**, 1087–1096.

Sane, S. P. & Jacobson, N. P. 2006 Induced airflow in flying insects II. Measurement of induced flow. *J. Expl Biol.* **209**, 43–56.

Wang, Z. J., Birch, J. B. & Dickinson, M. H. 2004 Unsteady forces and flows in low Reynolds number hovering flight: two-dimensional computations *vs.* robotic wing experiments. *J. Expl Biol.* **207**, 449–460.

Weis-Fogh, T. 1973 Quick estimates of flight fitness in hovering animals, including novel mechanisms for lift production. *J. Expl Biol.* **59**, 169–230.

Wu, J.-Z., Pan, Z.-L. & Lu, X.-Y. 2005 Unsteady fluid-dynamic forces solely in terms of control-surface integral. *Phys. Fluids* **17**, 098102.